Dynamics of photoexcited carriers and spins in InAsP ternary alloys

M. A. Meeker, B. A. Magill, T. R. Merritt, M. Bhowmick, K. McCutcheon, G. A. Khodaparast, J. G. Tischler, S. McGill, S. G. Choi, and C. J. Palmstrøm

Citation: Applied Physics Letters **102**, 222102 (2013); doi: 10.1063/1.4808346
View online: http://dx.doi.org/10.1063/1.4808346
View Table of Contents: http://scitation.aip.org/content/aip/journal/apl/102/22?ver=pdfcov
Published by the AIP Publishing

Dynamics of photoexcited carriers and spins in InAsP ternary alloys

M. A. Meeker,[1,a)] B. A. Magill,[1,a)] T. R. Merritt,[1] M. Bhowmick,[1] K. McCutcheon,[1] G. A. Khodaparast,[1,b)] J. G. Tischler,[2] S. McGill,[3] S. G. Choi,[4] and C. J. Palmstrøm[5]
[1]*Department of Physics, Virginia Tech, Blacksburg, Virginia 24061, USA*
[2]*Naval Research Laboratory, Washington, DC 20375, USA*
[3]*National High Magnetic Field Laboratory Florida, Tallahassee, Florida 32310, USA*
[4]*National Renewable Energy Laboratory, Golden, Colorado 80401, USA*
[5]*Department of Electrical and Computer Engineering, University of California, Santa Barbara, Santa Barbara, California 93106, USA*

(Received 30 April 2013; accepted 14 May 2013; published online 4 June 2013)

The recent rapid progress in the field of spintronics involves extensive measurements of carrier and spin relaxation dynamics in III-V semiconductors. In addition, as the switching rates in devices are pushed to higher frequencies, it is important to understand carrier dynamic phenomena in semiconductors on femtosecond time-scales. In this work, we employed time and spin resolved differential transmission measurements; to probe carrier and spin relaxation times in several InAsP ternary alloys. Our results demonstrate the sensitivity of the spin and carrier dynamics in this material system to the excitation wavelengths, the As concentrations, and temperature. © *2013 AIP Publishing LLC*. [http://dx.doi.org/10.1063/1.4808346]

Recently, g-factor engineering[1] has attracted much attention for potential applications in spintronics and in the case of InAsP ternary alloys, a wide range of g-factors, including $g = 0$, can be achieved. The recent rapid progress in the field of spintronics involves extensive measurements of carrier and spin relaxation dynamics in III-V semiconductors. In addition to spintronics applications, this material system is important for high-speed electronic as well as optoelectronic devices. Therefore, as the switching rates in devices are pushed to higher frequencies, it is important to understand carrier dynamic phenomena in semiconductors on femtosecond time-scales. In this work, we employed time and polarization-resolved differential transmission measurements to probe carrier and spin relaxation times in several InAsP ternary alloys.

InAsP is a ternary compound with characteristics between that of InAs and InP. The observed spin relaxation time in InP demonstrated tunability as a function of the carrier density, frequency, and intensity,[2–4] and can be on the order of tens of picoseconds at room temperature (RT)[2,3] in bulk InP, or hundreds of microseconds in charged quantum dots.[5] Several groups probed the spin life time in InAs using pump/probe spectroscopy, finding a spin life time of 24 ± 2 ps for nearly degenerate epitaxial layers of n-type InAs[6] and $\sim 19 \pm 4$ ps for intrinsic material.[7] Hall *et al.*[8] studied spin relaxation in (110) and (001) InAs/GaSb heterostructures and a spin lifetime of 18 ps was reported for (110) superlattices, much longer than that of the (001) structure with a life time of 700 fs. The large enhancement has been explained by the suppression of decay associated with asymmetry in interface bonding and bulk inversion asymmetry (BIA) contributions to the spin decay process in (110) superlattices. Litvinenko *et al.* measured spin lifetime in three undoped InAs films of different thicknesses (0.15, 0.27, and 1 μm) and for temperatures ranging from 77 K to 290 K.[9] Spin lifetimes of 1 and 20 ps were observed for 0.15 μm and 1 μm thick films, respectively, with the samples at 77 K. The measured spin relaxation time, using the magneto-optical Kerr effect spectroscopy in n-type InAs, demonstrated a strong dependence on the laser fluence with the time scale of the relaxation ranging from 1 to 5 ps.[10] Our results demonstrate sensitivity of the spin and carrier dynamics in $InAs_xP_{1-x}$ alloys to excitation wavelengths, As concentrations, and temperature.

In this work, $InAs_xP_{1-x}$ alloys with the compositions ranging from $x = 0.4$ to 0.75, grown on Fe-doped semi-insulating InP(001) by chemical beam epitaxy, were studied. The thicknesses of the $InAs_xP_{1-x}$ alloys vary from 4.3 to 5.5 μm, which is larger than the critical thickness for strain relaxation.[11] Details of the growth and structural properties are described in Ref. 11. In this study, we employed degenerate Time Resolved Differential Transmission (TRDT) pump/probe measurements where the laser source was an Optical Parametric Amplifier (OPA). The OPA itself was pumped by an amplified Ti:sapphire oscillator with a repetition rate of 1 KHz. The pump/probe pulses were tuned in the vicinity of the band gap and ranged from 1280 to 1350 nm. The pulses had a duration of $\sim$100 fs defining the resolution of the measurements with the ratio of the pump:probe of 1000:1. Both beams were focused onto the sample with a spot size of around 150–200 μm for probe and slightly larger for the pump. The differential transmissivity, as a function of the time delay between the pump and probe pulses using an InGaAs detector, was measured.

As a result of selection rules for interband transitions, spin-polarized carriers can be created using circularly polarized pump beams. By monitoring the transmission of a weaker, delayed probe pulse that has the same circular polarization (SCP) or opposite circular polarization (OCP) as the pump pulse, the optical polarization $P = (SCP - OCP)/(SCP + OCP)$ can be extracted. The optical polarization P decays exponentially

[a)]M. A. Meeker and B. A. Magill contributed equally to this work.
[b)]Author to whom correspondence should be addressed. Electronic mail: khoda@vt.edu.

with a decay constant related to the spin lifetime as following: $P = P_0 \exp(-t/\tau_s)$, where P_0 is a constant. Examples of our TRDT and Spin Polarized Differential Transmission (SPDT) are presented here, providing information on the carrier and spin relaxation time scale in this material system.

Figure 1(a) shows TRDT for $InAs_{0.75}P_{0.25}$ with the pump and probe $\lambda = 1280$–1350 nm, with an estimated photo-excited carrier density on the order of $1 \times 10^{19} cm^{-3}$. The TRDT shows several features, including a sharp change in transmission lasting for <1 ps, which can be attributed to a coherent artifact, commonly observed in a degenerate pump and probe scheme. The sharp increase is followed by a slower component which is dominated by photo-induced bleaching. Due to the *Pauli exclusion* principle, a large density of photo-excited electrons in the conduction band can reduce the amplitude of the interband optical absorption transitions via band and state filling. This leads to a decrease in the absorption, and a corresponding increase in the transmission, which is referred as photo-induced bleaching. The differential transmission can be written as: $\Delta T/T = e^{-(\alpha_0 - \alpha)L} - 1$, where T is the transmission, α_0 is the pre-excitation absorption coefficient, and L is the thickness of the sample.[12]

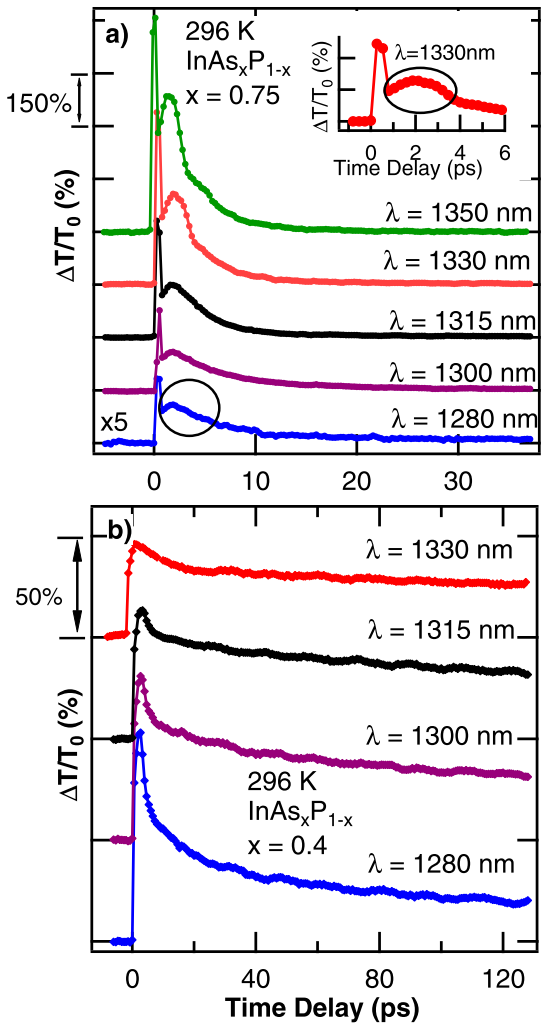

FIG. 1. Differential transmission of (a) $InAs_{0.75}P_{0.25}$, (b) $InAs_{0.40}P_{0.60}$ for different pump and probe wavelengths; the traces are offset for clarity. The inset shows an example of the initial temporal evolution τ_1, which can be attributed to the relaxation of the hot electrons through emission of LO-phonons. The time scale, denoted by τ_1, increases by increasing the excitation, and this increase is more pronounced for the sample with $x = 0.75$ than $x = 0.4$, where the excitation wavelengths for pump and probe are deeper in the conduction band.

In a thick optical medium, a small change in the absorption coefficient can accumulate to a large change in the transmission. The large photo-bleaching observed here can be expected since the sample thicknesses range from 4.3 to 5.5 μm. The relaxations of the photo-induced carriers in our samples can be modeled by two time constants, τ_1 and τ_2, where τ_1 is attributed to the initial carrier cooling and τ_2 to the relaxation time of hot electrons toward the bottom of the conduction band. The recombination time scales depend strongly on the As concentration, temperature, and the excitation wavelengths. In our carrier relaxation, the initial component of the temporal evolution can be attributed to the relaxation of the hot electrons. When a hot electron gas is created at room temperature, the carrier relaxation slows down since as the electron gas cools to the lattice, the lattice temperature rises, and subsequently, the number of equilibrium LO-phonons increase. In the regime of high electron densities, due to screening effects and hot phonons, the hot electrons experience a significant reduction in their energy loss rate through the emissions of LO phonons. Thus, we identify τ_1 as the thermalization time of the hot carriers which can be on the order of ~2–5 ps (as shown in the inset of Fig. 1(a) for $x = 0.75$ at 1330 nm), and τ_2 to the carrier relaxation time toward the bottom of conduction band, where the recombination time occurs on longer time scales depending on the As concentration and the excitation wavelength. Comparing the measurements presented in the inset of Fig. 1(a) at 1330 nm, for $InAs_{0.75}P_{0.25}$, to the measurements at the shorter wavelengths, we observed longer time scales for τ_1 with increasing excitation energy, where the increasing contribution of LO-phonons reduces the energy loss rate. The excitation energy dependence of τ_1 is more pronounced for the sample with a higher As concentrations where the excitation wavelengths for the pump and probe are deeper in the conduction band, compared to the measurements in Fig. 1(b) for $InAs_{0.4}P_{0.6}$.

In addition, as shown in Fig. 1(b), the carrier recombination time scale of $InAs_{0.4}P_{0.6}$ is much longer than the sample with $x = 0.75$. Time-resolved photoluminescence (TRPL) measurements allowed us to determine the carrier recombination time of $InAs_{0.4}P_{0.6}$, where photo-generated carrier lifetimes can be obtained by monitoring the transient PL signal after laser pulsed excitations. An example of the PL and the TRPL using a streak camera, for $InAs_{0.4}P_{0.6}$, are shown in Fig. 2. The excitation wavelength was fixed at 800 nm with a pulse duration of 100 fs and repetition rate of 1 KHz. The TRPL below 100 K in this sample demonstrated a recombination time on the order of ~1.0 ns with a weak temperature dependence.

Figure 3 shows the time scale of the carrier relaxations τ_2, at 296 K, for the samples with different As concentrations of $x = 0.4$, 0.6, 0.7, and 0.75, at different excitation wavelengths. We observed that the relaxation times for the sample with $x = 0.4$ are considerably different, ranging from 40 to 130 ps compared to ~2–6 ps for the samples with the higher

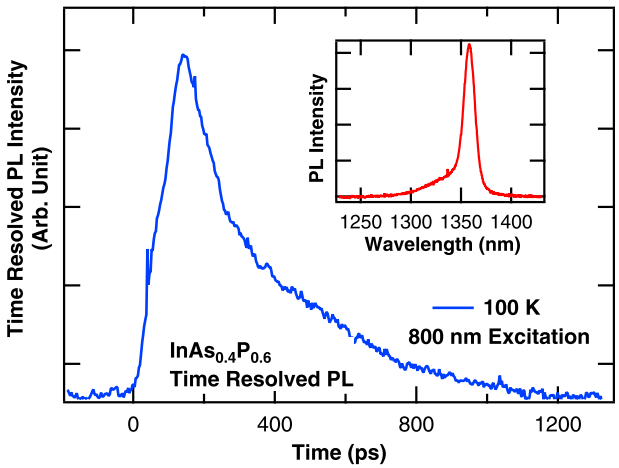

FIG. 2. Example of time resolved PL for $InAs_{0.4}P_{0.6}$ where the PL emission in this sample, as shown in the inset, was in the range detectable by a streak camera.

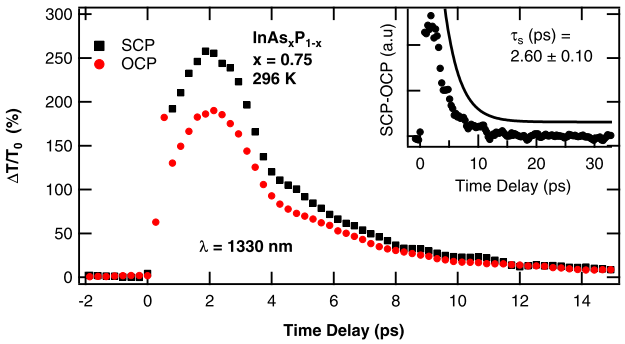

FIG. 4. Differential transmission of $InAs_{0.75}P_{0.25}$ for $\lambda = 1330$ nm excitation. SCP denotes data taken with the pump and the probe beams having the same circular polarization while OCP denotes them having opposite circular polarizations. Inset is SCP-OCP for the traces in the graph and the spin relaxation time was extracted by fitting an exponential to the SCP-OCP. The fit is shifted for clarity.

As concentrations. The long relaxation times for the sample with $x = 0.4$ are comparable to the carrier relaxation times previously observed in bulk InP.[2,3] The faster relaxation time in the sample with higher As concentrations could be related to higher defects states as well as increasing band mixing expected in the narrow gap band structures.

In order to probe the relaxation of photo-excited spin polarized carriers, two identical quarter wave plates were used to extract the SPDT for different pump/probe wavelengths. Figure 4 shows an example of the SPDT for $InAs_{0.75}P_{0.25}$, where the differential transmission for the pump and probe being SCP or OCP, were employed to calculate the spin relaxation time. As shown in the inset, by an exponential fit to the difference (SCP-OCP), the spin relaxation time can be extracted. The observed spin relaxation times for our sample structures are summarized in Fig. 5, where the longest spin relaxation was observed in the sample with $x = 0.4$, ranging from 20 to 60 ps. The observed spin relaxation times in the samples with the As concentration larger than 0.4 are comparable to the observations in InAs where the Elliot-Yaffet (EY)[13] mechanism can contribute to the relaxation process. In the EY picture, the strong mixing of the valence band states and conduction bands can result in non-zero transition rates even for spin-conserving scattering process.

In an undoped alloy structure, where equal number of holes and electrons are created after photo-excitation, several scattering mechanisms contribute to the spin relaxation, such as carrier-carrier, carrier-LO phonon and carrier-impurity scattering. The spin-lattice relaxation mechanism due to optical phonons does not work if phonon energy is much higher than the sample's temperature. When hot photo-excited electrons are created initially at low temperatures, there are no equilibrium optical phonons that can contribute to decrease

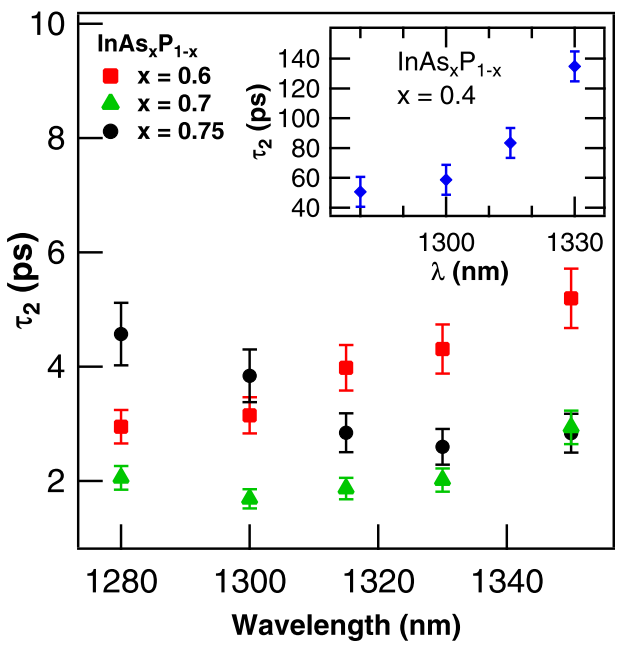

FIG. 3. Carrier relaxation time at 296 K, τ_2, versus λ for $InAs_xP_{1-x}$ with As concentrations $x = 0.6$, 0.7, and 0.75 extracted from the exponential fits. The inset shows τ_2 for $x = 0.4$.

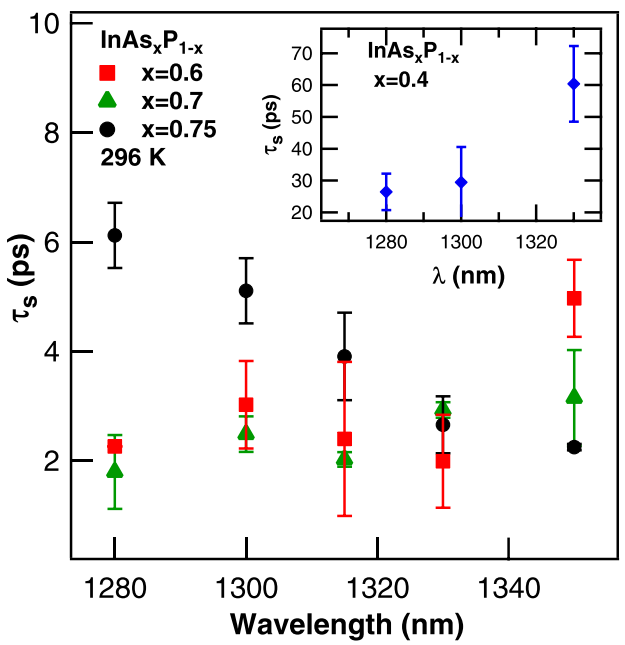

FIG. 5. Spin relaxation times (τ_s), obtained by the exponential fit of the difference between SCP and OCP curves, versus wavelength for $x = 0.6$, 0.7, and 0.75. The inset shows the spin relaxation time for $x = 0.4$, ranging from ~20 to 60 ps.

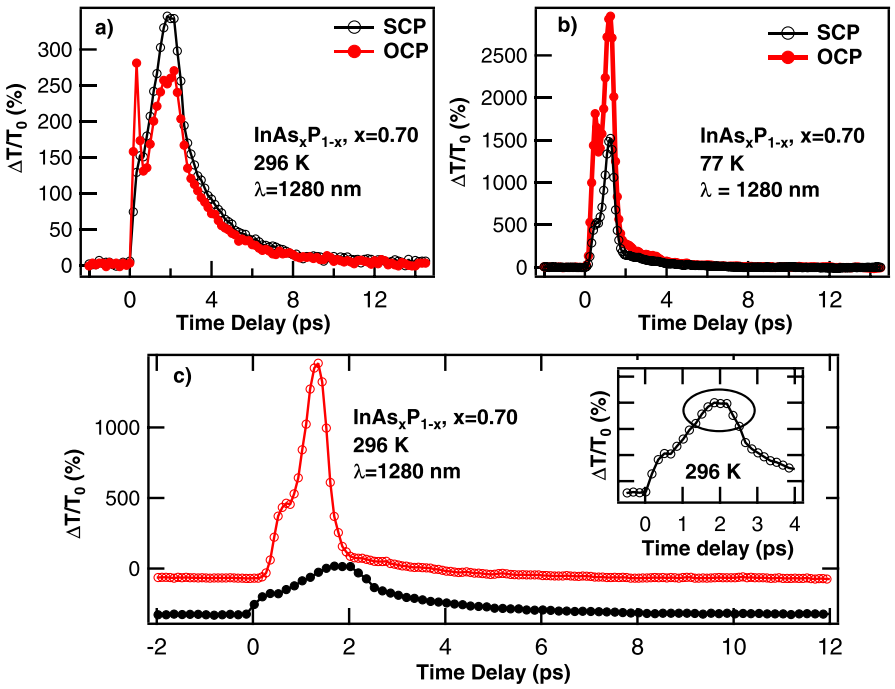

FIG. 6. Example of spin polarized differential transmission for the sample with $x = 0.7$ at 1280 nm for (a) RT and (b) 77 K. We observe much faster dynamics at 77 K. (c) Carrier relaxation times at RT and 77 K. The faster spin relaxations at 77 K are in concert with a faster relaxation of the photo-excited carriers. As shown in the inset, the initial component of carrier cooling is more important at RT.

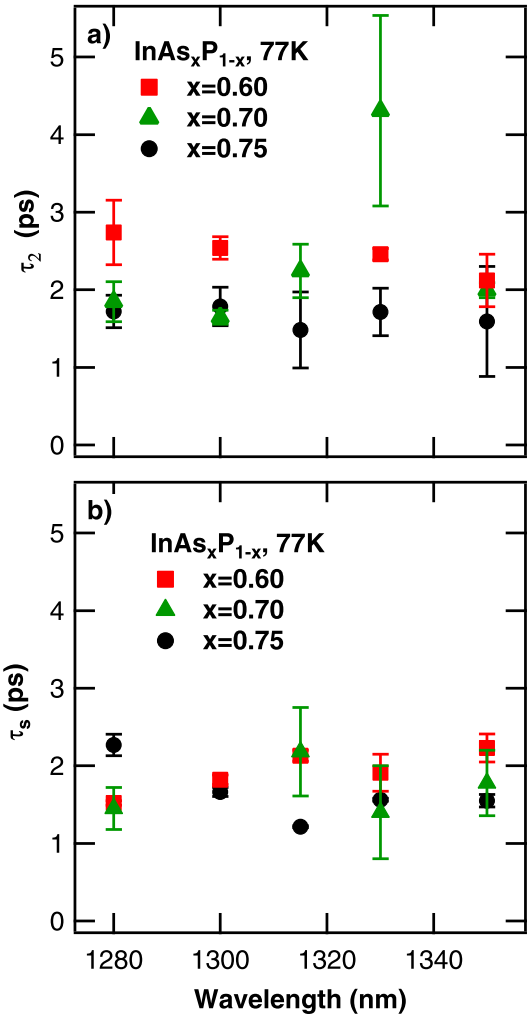

FIG. 7. (a) Time resolved and (b) spin resolved differential transmission. Both dynamics are faster at 77 K which could be due the absence of LO-phonons. When the hot photo-excited electrons are created initially at low temperatures, there are no equilibrium optical phonons that can contribute to the decrease of the relaxation rate. This fact can result in faster carrier relaxation times; it could also have resulted in the observed faster spin relaxations.

of the relaxation rate. As shown in Figs. 6(a) and 6(b), for the SPDT traces at RT and 77 K, we can observe faster spin relaxations at 77 K, in concert with faster carrier relaxation, as shown in Fig. 6(c), where the carrier relaxation time scales for RT and 77 K are compared.

The inset in Fig. 6(c) shows the initial cooling of hot electrons via emission of LO-phonons. In contrast, this component of the relaxation is insignificant at 77 K, and in our samples resulting in a faster spin relaxation time, consistent with the EY mechanism. A similar temperature dependence of spin relaxation for undoped (110) quantum wells (QWs) has been reported, suggesting the absence of Dyakonov-Perel (DP)[14] interaction, where the thermal ionization process of excitons with increasing temperature, was considered to be responsible for the increase of τ_s with temperature.[15] The summary of the carrier and spin relaxation times in our samples at 77 K, are presented in Fig. 7. Compared to the measurements at RT, the relaxations are faster by a factor of ~2. For the sample with $x = 0.4$ at 77 K, due to the increase in the band gap, only the pulses tuned at 1270 nm could have been employed and the carrier and spin relaxation times of ~29.0 ps and ~19.0 ps were extracted, respectively.

In summary, we have probed the dynamics of the photo-excited carriers and spins in $InAs_xP_{1-x}$ with different alloy compositions. Our results demonstrate the tunability of the time scales as a function of different external parameters. We observe several carrier relaxation components where the cooling of the photo-excited carriers, via the generation of LO phonons, play an important role and can contribute to the observed time scales of the carrier and spin relaxations in our sample structures.

This work was supported by NSF-Career Award No. DMR-0846834 and by the National High Magnetic Field Laboratory through a UCGP. G. A. Khodaparast thanks the inputs from Professor Tigran Shahbazyan and the funding from the Institute of Critical Technology and Applied

Sciences (ICTAS) at Virginia Tech. The samples studied in this work were grown and characterized as part of S. G. Choi's Ph.D. work at the University of Minnesota.

[1]H. Kosaka, A. A. Kiselev, F. A. Baron, K. W. Kim, and E. Yablonovitch, Electron. Lett. **37**, 464 (2001).
[2]H. Ma, Z. Jin, L. Wang, and G. Ma, J. Appl. Phys. **109**, 023105 (2011).
[3]B. Li, M. C. Tamargo, and C. A. Merilesa, Appl. Phys. Lett. **91**, 222114 (2007).
[4]C. P. Weber and E. A. Kittlaus, J. Appl. Phys. **113**, 053711 (2013).
[5]M. Ikezawa, B. Pal, Y. Masumoto, I. V. Ignatiev, S. Yu Verbin, and I. Ya. Gerlovin, Phys. Rev. B **72**, 153302 (2005).
[6]P. Murzyn, C. R. Pidgeon, P. J. Phillips, M. Merrick, K. L. Litvinenko, J. Allam, B. N. Murdin, T. Ashley, J. H. Jefferson, and L. F. Cohen, Appl. Phys. Lett. **83**, 5220 (2003).
[7]T. F. Boggess, J. T. Olesberg, C. Yu, M. E. Flatté, and W. H. Lau, Appl. Phys. Lett. **77**, 1333 (2000).
[8]K. C. Hall, K. Gündogdu, E. Altunkaya, W. H. Lau, M. E. Flatté, T. F. Boggess, J. J. Zinck, W. B. Barvosa-Carter, and S. L. Skeith, Phys. Rev. B **68**, 115311 (2003).
[9]K. L. Litvinenko, B. N. Murdin, J. Allam, T. Zhang, J. J. Harris, L. F. Cohen, D. A. Eustace, and D. W. McComb, Phys. Rev. B **74**, 075331 (2006).
[10]R. N. Kini, K. Nontapot, G. A. Khodaparast, R. E. Welser, and L. J. Guido, J. Appl. Phys. **103**, 064318 (2008).
[11]S. G. Choi, C. J. Palmstrøm, Y. D. Kim, D. E. Aspnes, H. J. Kim, and Y. C. Chang, Appl. Phys. Lett. **91**, 041917 (2007).
[12]J. Nunnenkamp, J. H. Collet, J. Klebniczki, J. Kuhl, and K. Ploog, Phys. Rev. B **43**, 14047 (1991).
[13]R. J. Elliot, Phys. Rev. **96**, 266 (1954).
[14]M. I. D'yakonov and V. I. Perel, Zh. Eksp. Teor. Fiz. **60**, 1954 (1971) [Sov. Phys. JETP **33**, 1053 (1971)]; Fiz. Tverd. Tela (Leningrad) **13**, 3581 (1971) [Sov. Phys. Solid State **13**, 3023 (1972)].
[15]Y. Ohno, R. Terauchi, T. Adachi, F. Matsukura, and H. Ohno, Phys. Rev. Lett. **83**, 4196 (1999).